

An improved STA/LTA algorithm for P wave detection in the 2015 Nepal Earthquake

Yuchen Wu^{1*}

* Yuchen Wu: Gulou District, Nanjing, Jiangsu, China; +86-181-51007758; wuy7268@gmail.com,

ABSTRACT:

Automatic identification of seismic phases is one of the important tasks in earthquake rapid reporting and early warning. The STA/LTA method is currently the most widely used automatic pickup method. However, the accuracy and stability of its pickup results heavily depend on the selection of feature functions, time window lengths, and trigger thresholds, so it is to some extent impossible to achieve automatic pickup of P-wave arrival time. We present an improved algorithm for automatically picking up P-wave arrival times. In this scheme, the weight factor K is introduced to construct a new feature function, and a method for finding the maximum value on the STA/LTA curve corresponding to the P-wave arrival time is proposed. This method was applied to measure the arrival of the 2015 Nepal Earthquake to validate previous evaluations. The results show that our improved method has the advantage of eliminating the time wasted on adjusting the trigger threshold when picking up the P-wave, which is necessary for the traditional STA/LTA method, and overcoming the challenge of inaccurate prediction when weak seismic signals with a low signal-to-noise ratio occur.

KEYWORDS: Earthquake Prediction, Seismic Monitoring, STA/LTA, Automatic Picking of P-Wave, Nepal Earthquake

1 INTRODUCTION

On April 25, 2015, a devastating earthquake with a magnitude of 7.8 struck Nepal, destroying buildings and profound disruption to the lives of its citizens^[15]. From a historical perspective, the first major earthquake in Nepal was recorded on June 7, 1255, with an estimated magnitude of approximately 7.7 on the Richter scale. During that catastrophe, Kathmandu lost a third of its population. Five years later, in 1260, another significant earthquake caused extensive damage to numerous structures. In either August or September of 1408, Kathmandu was again shaken by a major earthquake. Unfortunately, there is limited information about the earthquake in 1681, but it also claimed numerous lives and caused extensive damage to buildings. In either June or July of 1767, Nepal experienced yet another earthquake. Within 24 hours, this major seismic event unleashed 21 earthquakes and aftershocks. Records also indicate significant earthquakes in 1810, 1823, 1833, 1834, and 1883. The most recent earthquake before the 2015 Nepal earthquake is believed to be the one that occurred in 1934, claiming the lives of over 8,500 Nepalese people.

From a geological perspective (see Figure 1), the ongoing collision between the Indo-Australian plate and the Eurasian plate, which began approximately 50 million years ago, has made Nepal and the entire Himalayan range one of the most seismically active regions on Earth^[5]. The

2015 earthquake in Nepal was triggered by the geological stress that accumulated along the Himalayas. Here, the crustal plate carrying India collides with and subducts beneath the central Asian crust at a rate of 4-5 centimeters per year^[15]. Because the motion of India towards Asia occurs nearly perpendicular to the Himalayan Mountains in Nepal, this earthquake resulted from thrust faulting (reverse faulting) between the subducting Indo-Australian Plate and the overriding Eurasian Plate to the north^[5].

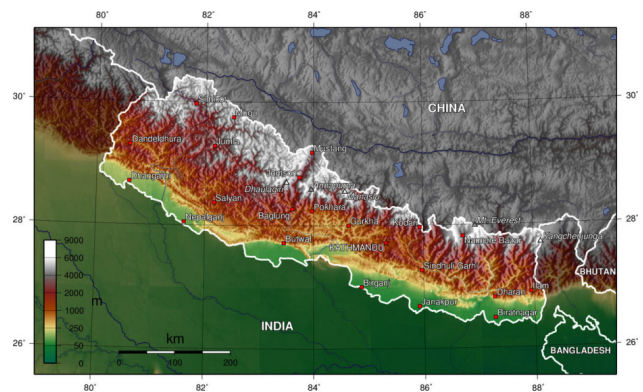


Figure 1 Geologic map of Nepal

https://en.wikipedia.org/wiki/Geology_of_Nepal

The prediction of earthquakes has long been a prominent topic for measuring earthquake magnitudes and guiding post-disaster rescue efforts. The initial ground movement is primarily generated by P-waves, which

are observable. Subsequently, P-waves are utilized to predict the ground motion caused by the later arrival of S-waves and surface waves^[12]. Methods employed for P-wave identification include the AIC criterion method, autoregressive prediction, neural network methods, and the STA/LTA method. The AIC criterion method, grounded in information theory, boasts a robust statistical foundation and can be justified as Bayesian, incorporating a sophisticated prior model that accounts for sample size and the number of model parameters^[2]. This method is particularly accurate in timing P-wave arrivals. However, this method is only suitable for the initial seismic wave whose location is roughly known^[4]. In addition, the AIC method is not useful for practical alerts of $M_w \leq 8$ earthquakes, and in the last 50 years, 24 $M_w > 8.0$ earthquakes occurred, of which 5 with $M_w \geq 8.5$ and 2 with $M_w \geq 9$ (<https://earthquake.usgs.gov/earthquakes/search/>). Applying the AIC method to identify potential ionospheric pre-seismic signals is challenging, as it tends to produce too many false alarms, rendering it impractical^[13]. The autoregressive prediction method involves establishing a regression equation for prediction by leveraging the dependency relationship between the historical time series of the prediction target and its values at different time intervals^[1]. While this method offers high accuracy, it suffers from slow computation speed^[7]. A neural network model comprises numerous interconnected processing units (neurons) that enable information processing through their interactions. Knowledge and information storage manifest as network component interconnections and distributed physical information connections. While the neural network method exhibits broad applicability, it is characterized by complex calculations and extended processing times^[13, 17]. The traditional STA/LTA method calculates the ratio of short-term average (STA) energy within a brief time window to long-term average (LTA) energy within a more extended time window, with these windows continuously shifting through the data stream. Detection is declared when the STA/LTA ratio surpasses predefined thresholds^[15]. However, this method necessitates manual adjustment of the trigger threshold value, which can be time-consuming, particularly in post-earthquake rescue operations^[13]. Therefore, we will introduce the enhanced STA/LTA method for earthquake prediction. This method is expected to offer several advantages, including eliminating the time-consuming threshold adjustment and improved result accuracy^[6]; this method will also be applied to simulate the prediction of the 2015 Nepal Earthquake to test its stability and noise resistance.

2 METHODOLOGY

The traditional method of STA/LTA was first detected by Stevens^[8]. STA mainly reflects the average energy of seismic signals, while LTA specifically reveals the average energy of background noise. When the seismic signal arrives, the STA/LTA changes rapidly, and the corresponding STA/LTA value will significantly increase. The moment when its value exceeds the preset trigger threshold can be determined to be the arrival time of the P-wave^[14]. The trigger and retrigger thresholds are commonly considered equal and called the detection threshold ($\tau > 1$), although they can differ. Thus, the most important STA/LTA trigger algorithm parameters are the STA and LTA window lengths (NS and NL), and the detection threshold (τ)^[16].

Considering the traditional method of STA/LTA (Formulas (1) (2) and (3)), i represents the sampling time. Long represents the length of the long-term window. Short represents the length of the short-term window. λ indicates the preset trigger threshold. $CF(i)$ represents the characteristic function value of the seismic signal at the time i , revealing the changes in amplitude and energy of the seismic data^[6].

$$LTA(i) = \frac{1}{\text{long}} \sum_{j=i}^{i+\text{long}} CF(j) \quad (1)$$

$$STA(i) = \frac{1}{\text{short}} \sum_{j=i+\text{long}}^{i+\text{long}+\text{short}} CF(j) \quad (2)$$

$$\frac{STA}{LTA}(i) = \frac{STA(i)}{LTA(i)} \geq \lambda \quad (3)$$

The improved STA/LTA method creates a new characteristic function by introducing the weighting factor K ^[1]. In the formulas, the weighting factor K is the allocation of signal amplitude and frequency weights based on the signal sampling frequency and the inherent noise properties of the station. ω represents the amplitude characteristics of the signal, while f represents the frequency characteristics of the signal. Therefore, this feature function contains detailed signal amplitude and frequency parameter characteristics. When a seismic event occurs, either or both the amplitude and frequency of the signal will undergo a sudden change. The feature function “F” can accurately reflect these changes and respond swiftly^[6].

The following two formulas illustrate two essential processes. Formula (4) represents the first process, which involves introducing the weight factor K . To achieve this, we calculate the sum of the absolute values of the signal in a real seismic signal sequence, denoted as x_i . Subsequently, we find the first derivative of the signal,

sum the absolute values of the first derivative, and consider the ratio of these two sums as the weight factor K. Formula (5) signifies the second process, which is the construction of a feature function. The significant information contained within the signal encompasses aspects such as energy, frequency changes, and amplitude. We use the weight factor to construct the feature function $F^{[6]}$ to leverage these signal characteristics.

This method has a strong matched-filter technique, which is of great help in overcoming the challenge of weak seismic signals with low signal-to-noise ratio^[3]. Then the data will be imported into MATLAB to form graphs of the acceleration of the P-wave and two spectrograms of its frequency.

$$K = \frac{\sum_{i=1}^{len} |X(i)|}{\sum_{i=1}^{len} |X'(i)|} \quad (4)$$

$$F = X(i+1)^2 + K(X(i+1) - X(i))^2 \quad (5)$$

3 RESULTS

On April 25, 2015, at 11:56 AM, a magnitude 7.8 earthquake, known as the Gorkha earthquake, struck. It had its epicenter located 77 km (48 miles) northwest of Kathmandu in the village of Barpak, Gorkha district (Latitude 28.240 degrees, Longitude 84.750 degrees) (see Figure 2). The duration of strong shaking during this earthquake was approximately 40 seconds, as recorded by the Department of Mining and Geology. The earthquake's mechanism was characterized as a low-angle thrust reverse fault. Subsequently, there were approximately 367 aftershocks^[5].

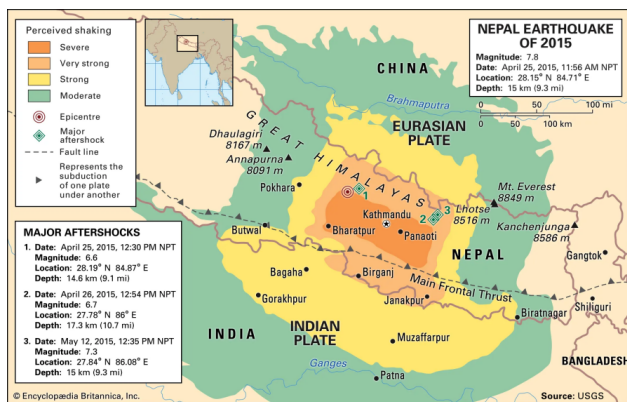


Figure 2 The epicenter of Nepal earthquake
<https://www.britannica.com/topic/Nepal-earthquake-of-2015#/media/1/2024843/197923>

The improved method is utilized to review the process of the 2015 Nepal Earthquake to test its feasibility. The new method analyzes the data and creates Figure 3 below. The figure shows three subplots where the first plot

reveals P-wave arrival detection by our improved STA/LTA method, marked by the green line. The second plot depicts the spectrogram with almost appropriate detection of the P-wave first arrival marked by the green line. The third plot displays the same spectrogram with a -50dB threshold applied to get a clear view of the first P-wave arrival. From the three subplots, it is concluded that the first P-wave reaches the detector at 32 seconds. Since the three subplots can be concluded in one figure within 10 seconds after the real-time data input, it can be efficient enough for the safe evacuation before the earthquake and rescue activities afterward.

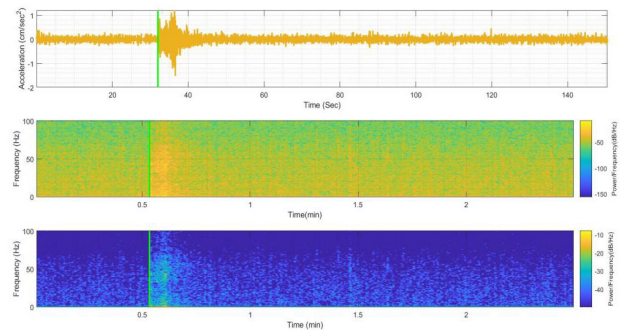


Figure 3 Acceleration of P-wave and its frequency

4 CONCLUSIONS

The improved STA/LTA method detects the impulse of the earthquake in a shorter period. It can reveal the arrival of the P-wave vividly by analyzing the changes in the acceleration of the P-wave and depicting spectrograms of frequency. In this way, a clearer view of the first P-wave arrival will be obtained. In the future, this method can be applied to identify all of the earthquake hazards and risk areas in advance, assisting in outlining more appropriate ways of safe evacuation before the earthquake and the rescue activities afterward.

REFERENCES

1. Bai, Y., Jin, X., Wang, X., Su, T., Kong, J., & Lu, Y. (2019). Compound autoregressive network for prediction of multivariate time series. *Complexity*, 2019, 1-11.
2. Burnham, K. P., & Anderson, D. R. (2004). Multimodel inference: understanding AIC and BIC in model selection. *Sociological methods & research*, 33(2), 261-304.
3. Grigoli, F., Cesca, S., Krieger, L., Kriegerowski, M., Gammaldi, S., Horalek, J., ... & Dahm, T. (2016). Automated microseismic event location using master-event waveform stacking. *Scientific reports*, 6(1), 25744.
4. Hendriyana, A., Bauer, K., Muksin, U., & Weber, M. (2018). AIC-based diffraction stacking for local earthquake locations at the Sumatran Fault (Indonesia). *Geophysical Journal*

- International, 213(2), 952-962.
5. Hossain, A. S. M. F., Adhikari, T. L., Ansary, M. A., & Bari, Q. H. (2015). Characteristics and consequence of Nepal earthquake 2015: a review. *Geotechnical Engineering Journal of the SEAGS & AGSSFA*, 46, 114-20.
6. LIU Xiao-ming, ZHAO Jun-jie, WANG Yun-min, PENG Ping-an. Automatic Picking of Microseismic Events P-wave Arrivals Based on Improved Method of STA/LTA[J]. *Journal of Northeastern University:Natural Science*, 2017, 38(5): 740-745.
7. Perol, T., Gharbi, M., & Denolle, M. (2018). Convolutional neural network for earthquake detection and location. *Science Advances*, 4(2), e1700578.
8. Saqib, M., Şentürk, E., Sahu, S. A., & Adil, M. A. (2021). Ionospheric anomalies detection using autoregressive integrated moving average (ARIMA) model as an earthquake precursor. *Acta Geophysica*, 69(4), 1493-1507.
9. Stevens, J. L., & Adams, D. A. (2000, September). Improved surface wave detection and measurement using phase-matched filtering and improved regionalized models. In *Proceedings of the 22nd Annual DoD/DOE Seismic Research Symposium* (Vol. 1, pp. 145-154).
10. Tozzi, R., Masci, F., & Pezzopane, M. (2020). A stress test to evaluate the usefulness of Akaike information criterion in short-term earthquake prediction. *Scientific reports*, 10(1), 21153.
11. Trnkoczy, A. (2009). Understanding and parameter setting of STA/LTA trigger algorithm. In *New manual of seismological observatory practice (NMSOP)* (pp. 1-20). Deutsches GeoForschungsZentrum GFZ.
12. Vaezi, Y., & Van der Baan, M. (2015). Comparison of the STA/LTA and power spectral density methods for microseismic event detection. *Geophysical Supplements to the Monthly Notices of the Royal Astronomical Society*, 203(3), 1896-1908.
13. VOHRADSKY, J. (2001). Neural network model of gene expression. *the FASEB journal*, 15(3), 846-854.
14. WANG Yi-ying, DING Ren-wei, LI Jian-ping, ZHAO Li-hong, ZHAO Shuo, ZHANG Shuo-wei. Automatic pickup of microseismic P-wave arrival based on improved STA/LTA and MLoG operators. *Journal of Shandong University of Science and Technology: Natural Science*, 2021, 40(6): 1-10.
15. Witze, A. (2015). Major earthquake hits Nepal. *Nature*, 10.
16. Wu, Y. M., & Zhao, L. (2006). Magnitude estimation using the first three seconds P-wave amplitude in earthquake early warning. *Geophysical research letters*, 33(16).
17. Yoon, C. E., O'Reilly, O., Bergen, K. J., & Beroza, G. C. (2015). Earthquake detection through computationally efficient similarity search. *Science advances*, 1(11), e1501057.